Solid State Sciences xxx (2009) 1–4

Contents lists available at ScienceDirect

Solid State Sciences

journal homepage: www.elsevier.com/locate/ssscie

Electromechanical properties of single domain PZN–12%PT measured by three different methods

Guennou Mael[a,*], Dammak Hichem[a], Djémia Philippe[b], Moch Philippe[b], Pham-Thi Mai[c]

[a] Laboratoire SPMS, UMR 8580 CNRS, École Centrale Paris, Grande Voie des Vignes, 92295 Châtenay-Malabry, France
[b] LPMTM CNRS (UPR 9001), Université Paris 13, 93430 Villetaneuse, France
[c] Thales Research & Technology France, 91767 Palaiseau, France

ARTICLE INFO

Article history:
Received 19 January 2009
Received in revised form
20 February 2009
Accepted 18 March 2009
Available online xxx

Keywords:
Piezoelectricity
Resonance–antiresonance method
Brillouin scattering
Resonant ultrasound spectroscopy

ABSTRACT

In this paper, we compare the electromechanical properties of tetragonal single domain PZN–12%PT single crystals obtained by different methods: resonance–antiresonance method, Brillouin scattering, and resonant ultrasound spectroscopy. The agreement between the different measurements is found satisfactory for many elastic constants within experimental uncertainties. Differences are notable for the elastic constants associated to the propagation of shear waves (c_{66}^E and c_{44}^E). This can be accounted for by imperfections of the sample in acoustic spectroscopy and specific difficulties of shear resonators used for the resonance method. Strong discrepancies are noted for the hardened elastic constant c_{33}^D associated to longitudinal waves propagating along the polarization direction; we suggest this can arise from a frequency dependence of the dielectric constant.

1. Introduction

$Pb(Zn_{1/3}Nb_{2/3})O_3$–$xPbTiO_3$ (PZN–xPT) and $Pb(Mg_{1/3}Nb_{2/3})O_3$–$xPbTiO_3$ (PMN–xPT) single crystals have raised considerable interest for more than 10 years due to their excellent piezoelectric properties, which offer promising improvement perspectives for piezoelectric transducers and actuators. In those systems, the highest piezoelectric coefficients d_{33} are obtained for compositions close to the morphotropic phase boundary ($x \approx 9\%$ for PZN–xPT, 35% for PMN–xPT) when poled along a [001] direction [1]. The electromechanical properties of such crystals are fully characterized by a piezoelastic tensor that consists in elastic, piezoelectric and dielectric constants. The accurate determination of the constants is essential from a practical point of view for the prediction of device performances, as well as for a proper understanding of the different contributions and mechanisms that come into play.

The aim of this study is to measure the electromechanical properties of tetragonal single domain PZN–12%PT by different methods and discuss the discrepancies observed. The paper is organized as follows. Section 2 describes the sample preparation, Section 3 describes the different measurements performed. The results are then compared and discussed in Section 4.

2. Sample preparation

PZN–12%PT single crystals were grown by the flux method (PbO flux) as described elsewhere [2]. They are orientated using the Laue back-scattering technique. Crystals are cut with a wire saw along appropriate crystallographic directions. Crystal faces are polished on silicon carbide disks with grain sizes down to 1 μm to obtain mirror-like surfaces. Gold electrodes (not thicker than 0.15 μm) are sputtered on the relevant surfaces of the samples. Samples are then annealed at 400 °C for 2 h to release stress induced by polishing. The crystals are poled by the field cooling method whereby the sample is heated up into the cubic phase (490 K), an electric field is applied along a [001] direction and the sample is slowly cooled down. For all samples, we used an electric field of 1 kV/cm and a cooling rate of 2 °C/min.

PZN–12%PT crystals are tetragonal with a spontaneous polarization lying along a [001] direction [3]. When poled along one of the 6 equivalent directions, the crystal is in a tetragonal single domain state labelled 1 T with macroscopic symmetry 4 mm. We had previously shown that the single domain state could be unstable in plates thinner than 300 μm [4] and checked by optical microscopy that the polarization is homogeneous throughout the samples. In the single domain state, the electromechanical properties are then fully characterized by 11 independent coefficients. Choosing the stress T_λ and electric field E_i as independent variables, they are divided into 6 elastic constants s_{11}^E, s_{12}^E, s_{13}^E, s_{33}^E, s_{55}^E and s_{66}^E,

* Corresponding author.
E-mail address: mael.guennou@supaero.org (M. Guennou).

1293-2558/$ – see front matter © 2009 Elsevier Masson SAS. All rights reserved.
doi:10.1016/j.solidstatesciences.2009.03.026

3 piezoelectric constants d_{31}, d_{33} and d_{15} and 2 dielectric constants ${\varepsilon_{11}}^T$ and ${\varepsilon_{33}}^T$.

3. Measurements of electromechanical properties

3.1. Resonance–antiresonance method

The resonance–antiresonance method is widely used for the characterization of piezoelectric crystals and ceramics. Depending on the symmetry, measurements of a sufficient number of samples with different cuts can yield the full piezoelastic tensor. For a crystal with a 4 mm symmetry, the 11 independent coefficients of the piezoelastic tensor can be obtained from impedance measurements of samples in 5 geometries as described by Geng et al. [5]. All geometries with orientations and approximate dimensions are listed in Table 1, as well as the constants obtained directly from each sample. The remaining constants can be calculated by making use of the relations between piezoelastic constants [6]:

$$
\begin{aligned}
e_{33} &= k_{t33}\sqrt{\varepsilon_{33}^S c_{33}^D} \\
e_{31} &= \frac{\varepsilon_{33}^T - \varepsilon_{33}^S - d_{33}e_{33}}{2d_{31}} \\
s_{13}^E &= \frac{d_{33} - e_{33}s_{33}^E}{2e_{31}} \\
s_{12}^E &= -s_{11}^E + \frac{2\left(s_{13}^E\right)^2}{s_{33}^E - 1/c_{33}^E} \\
s_{66}^E &= 4s_{11}^{E*} - 2\left(s_{11}^E + s_{12}^E\right)
\end{aligned}
$$

The $c_{\alpha\beta}^E$ needed for comparison with other measurements are then calculated as the inverse of $s_{\alpha\beta}^E$.

Impedance measurements are carried out at room temperature with an impedance analyzer HP 4294A. The samples resonate in the 100 kHz range for transverse and length extensional modes and in the MHz range for thickness modes. The dielectric constants at constant stress ε^T are calculated from capacitance measurements at low frequency (1 kHz). The results are reported in Table 2.

3.2. Brillouin scattering

Brillouin scattering is inelastic scattering of light by acoustic waves. It is a standard method for the determination of elastic constants of transparent purely elastic materials. The full description of the measurements needed for usual symmetries was given by Vacher and Boyer [7]. Measurements of piezoelastic tensors by Brillouin scattering have been reported for the classical piezoelectric perovskites $BaTiO_3$ [8], $PbTiO_3$ [9] and $KNbO_3$ [10] and more recently for PZN–4.5%PT poled along [111] (single domain state) [11] and PMN–33%PT poled along [001] (multidomain state) [12].

Brillouin scattering along high symmetry directions only cannot yield the full piezoelastic tensor. It is usually necessary to measure the full dispersion in a set of planes and fit the elastic, piezoelectric and dielectric constants. In addition, an independent measurement of the dielectric constants in the frequency range of the Brillouin shifts is recommended [9].

In this work, we restricted our work to scattering along special directions. This yields the four constants ${c_{11}}^E$, ${c_{12}}^E$, ${c_{66}}^E$, ${c_{33}}^D$ and the two refraction indexes n_o and n_e.

We used a monomode argon laser ($\lambda = 514$ nm). The power of the laser on the sample was maintained below 100 mW to avoid heating of the samples during the measurement. Three different samples were used. Their orientations and approximate dimensions are listed in Table 2.

We use two different geometries. In the first geometry, the laser beam is normal to the crystal plane (back-scattering geometry). In the second geometry, the laser beam makes an incidence angle of 60° (platelet geometry). For back-scattered light, the relation between the velocity $V = \sqrt{c/\rho}$ of the elastic wave and the Brillouin shift Δf is

$$V = \frac{\lambda \Delta f}{2n} \tag{1}$$

where the refraction index n is chosen according to the laser propagation and polarization directions. In this configuration, for a laser light propagating along a high symmetry direction, only the longitudinal mode is expected to be Brillouin active. The spectra exhibit a single peak (Stokes and anti-Stokes) corresponding to this mode. The measurements of the Brillouin shifts for laser directions along [100], [110] and [001] give us the ${c_{11}}^E$, the combination $({c_{11}}^E + {c_{12}}^E + 2{c_{66}}^E)/2$ and ${c_{33}}^D = {c_{33}}^E + {e^2}_{33}/{\varepsilon_{33}}^S$ respectively.

In the platelet geometry, in addition to the light back-scattered from the beam refracted in the sample, we collect light that is scattered by elastic waves propagating in the plane of the plate. For the latter, the relation between V and Δf becomes

$$V = \frac{\lambda \Delta f}{2\sin\alpha} \tag{2}$$

where α is the incidence angle of the laser on the plate. Remarkably, the Brillouin shift is then independent of the refraction index. Measuring the same wave in both back-scattering and platelet geometry enables us to estimate the refraction index. Values for both ordinary and extraordinary indexes n_o and n_e can be found by choosing appropriate polarization directions for the laser.

To analyze the back-scattered light in the platelet geometry, we need to consider the general case of an elastic wave propagating in the (001) plane, with wave vector $k = (\cos\theta, \sin\theta, 0)$. The angle θ is the angle between the normal to the plane and the propagation direction of the laser beam in the sample. It is related to the incidence angle α of the plate by the Snell–Descartes relation $n\sin\theta = \sin\alpha$. The Christoffel tensor for this general direction reads

$$
\begin{pmatrix}
c_{11}^E\cos^2\theta + c_{66}^E\sin^2\theta & (c_{12}^E + c_{66}^E)\sin\theta\cos\theta & 0 \\
(c_{12}^E + c_{66}^E)\sin\theta\cos\theta & c_{66}^E\cos^2\theta + c_{11}^E\sin^2\theta & 0 \\
0 & 0 & c_{44}^E + e_{15}^2/\varepsilon_{11}^S
\end{pmatrix}.
$$

Selection rules indicate that the purely transverse wave polarized along the c-axis cannot be seen [7]. Only the quasi-longitudinal and

Table 1
Description of the samples used for impedance measurements. Polarization direction is [001] for all samples. Dimensions are approximate.

Mode	Orientation	Dimensions	Constants obtained
Transverse extensional	[100] × [010] × [001]	$5 \times 1 \times 0.5$ mm^3	k_{31}, s_{11}^E, d_{31}
Transverse extensional	[110] × [1$\bar{1}$0] × [001]	$5 \times 1 \times 0.5$ mm^3	$s_{11}^{E*} = (1/4)s_{66}^E + (1/2)(s_{11}^E + s_{12}^E)$
Length extensional	[001] × [100] × [010]	$5 \times 1 \times 1$ mm^3	k_{33}, s_{33}^D, d_{33}
Plate thickness	[100] × [010] × [001]	$6 \times 6 \times 0.3$ mm^3	k_{t33}, c_{33}^D, e_{33}
Shear thickness	[001] × [010] × [100]	$5 \times 5 \times 0.3$ mm^3	k_{t15}, c_{33}^D, e_{15}

Please cite this article in press as: M. Guennou, H. Dammak, et al., Electromechanical properties of single domain PZN–12%PT measured by three different methods, Solid State Sci. (2009), doi:10.1016/j.solidstatesciences.2009.03.026

Table 2
Description of the samples used for Brillouin scattering. Polarization direction is [001].

	Length × width × thickness	Dimensions
A	[100] × [010] × [001]	$3 \times 3 \times 0.4$ mm^3
B	[001] × [010] × [100]	$3 \times 3 \times 0.4$ mm^3
C	[001] × [110] × [1$\bar{1}$0]	$6 \times 3 \times 1$ mm^3

the quasi-transverse modes are Brillouin active. More precisely, it can be checked from the Christoffel tensor that their elastic moduli ρV^2 satisfy the relation $\rho V_{ql}^2 + \rho V_{qt}^2 = {c_{11}}^E + {c_{66}}^E$. The measurement of a spectrum therefore yields the combination ${c_{11}}^E + {c_{66}}^E$. A typical spectrum in the platelet geometry is given Fig. 1.

Table 3 summarizes the different cases. The final results are reported in Table 4.

3.3. Resonant ultrasound spectroscopy

In resonant ultrasound spectroscopy (RUS), the piezoelastic tensor is fitted to reproduce the resonance modes of a cubic sample identified by laser interferometry. All the details of the method as well as the full results have been published previously in Ref. [13]. The final results for PZN–12%PT in its single domain state are reported in Table 4.

4. Discussion

All measurements are compared in Table 4. We also report some values obtained by Zhang et al. [14] by the resonance method. Their results and our own resonance measurements are found in good agreement.

Let us focus on the results obtained by the resonance–anti-resonance method first. We notice that some coefficients are given with a very large uncertainty, especially ${c_{12}}^E$, ${c_{13}}^E$ and ${c_{66}}^E$. This originates from the fact that those coefficients are not obtained by direct measurements but indirectly by calculation using the piezoelectric constitutive equations. Similar issues have been

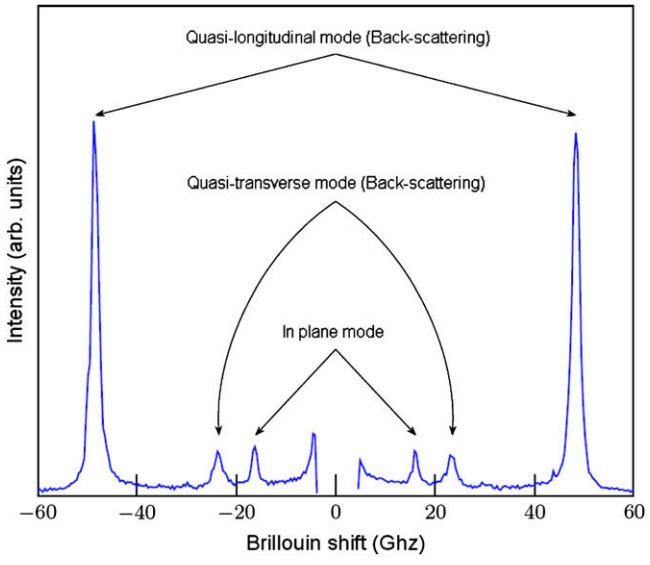

Fig. 1. Typical Brillouin spectrum obtained in the platelet geometry (incidence angle = 60°). The two modes at higher Brillouin shifts correspond to back-scattering processes. The last one is a longitudinal mode propagating in the plane of the plate. All other modes are forbidden by selection rules.

Table 3
For each constant or combination of constants, the different geometries used are listed. "BS" and "plate" refer respectively to back-scattering and scattering from a wave propagating in the plane of the plate. The refraction index appears for back-scattered light in equation (1). It is chosen according to the polarization direction of the laser.

Coefficient	Sample	Incidence	Mode	Index
c_{11}^E	A	60°	Plate	
	B	0°	BS	n_e
	B	0°	BS	n_o
	B	60°	Plate	
$(c_{11}^E c_{12}^E 2c_{66}^E)/2$	C	0°	BS	n_e
	C	0°	BS	
	C	60°	Plate	
c_{11}^E c_{66}^E	C	60°	BS	n_e
	B	60°	BS	n_e
$c_{33}^E + e_{33}^2/\varepsilon_{33}^S = c_{33}^D$	A	0°	BS	n_o
	C	60°	Plate	
	B	60°	Plate	

Refraction indexes at $\lambda = 514$ nm: $n_o = 2.69$; $n_e = 2.66$.

pointed out by Jiang et al. [15]. Nonetheless, the agreement is good for most elastic constants at constant electric field $c_{\alpha\beta}^E$.

The agreement however is not satisfactory for ${c_{55}}^E$ and ${c_{66}}^E$, both related to the propagation of shear waves. A reason for this might be the cracks observed in the sample used for RUS and mentioned in Ref. [13]. This might also explain why the electromechanical coupling coefficients determined by RUS are slightly lower than the values obtained from resonance measurements. As far as the determination of ${c_{55}}^E$ by the latter method is concerned, it must be highlighted that a decoupling of the thickness shear mode requires a much higher length to thickness ratio than for other vibration modes (about 20) [16]. Our samples did not quite reach this requirement, resulting in a non pure shear mode and thus higher uncertainties for the elastic constant ${c_{55}}^E$ (determined from the antiresonance frequency), the electromechanical coefficient k_{15} and

Table 4
Elastic constants ($c_{\alpha\beta}^E$ or $c_{\alpha\beta}^D$), dielectric constants (ε_{ij}^T or ε_{ij}^S) and piezoelectric constants ($d_{i\alpha}$ or $e_{i\alpha}$) for PZN–12%PT obtained by different methods.

	Brillouin (this work)	Resonance (this work)	RUS (Ref. [13])	Resonance (Ref. [14])
k_{31}		54.6 ± 2	47	54%
k_{33}		87.8 ± 1	67	87%
k_{t33}		60.0 ± 1	25	55%
k_{15}		49.7 ± 3		%
c_{11}^E	153 ± 1	157 ± 20	152 ± 2	GPa
c_{12}^E	83 ± 4	117 ± 30	87 ± 1	GPa
c_{13}^E		92 ± 30	90 ± 0.5	GPa
c_{33}^E		80 ± 5	84 ± 2	GPa
c_{55}^E		51 ± 5	37 ± 3	GPa
c_{66}^E	72 ± 2	58 ± 53	22 ± 1	GPa
c_{33}^D	147 ± 2	125 ± 6	89	GPa
d_{31}		-207 ± 10	-158	-207 pm/V
d_{33}		541 ± 30	386	560 pm/V
d_{15}		653 ± 100	946	pm/V
e_{31}		-1.7	-3 ± 0.5	C/m^2
e_{33}		8.2	4 ± 1	C/m^2
e_{15}		33.5	35 ± 3	C/m^2
ε_{11}^T		$10\,000 \pm 500$	6160	ε_0
ε_{33}^T		750 ± 50	612	$870\varepsilon_0$
ε_{11}^S		7530	2420 ± 150	ε_0
ε_{33}^S		170	331 ± 50	$211\varepsilon_0$

Please cite this article in press as: M. Guennou, H. Dammak, et al., Electromechanical properties of single domain PZN–12%PT measured by three different methods, Solid State Sci. (2009), doi:10.1016/j.solidstatesciences.2009.03.026

eventually for $d_{15} = k_{15}\sqrt{\varepsilon_{11}^{T}/c_{55}^{E}}$. The discrepancies can most probably be accounted for by such technical difficulties.

The discrepancy is also significant for the so-called "hardened" elastic constant $c_{33}{}^{D} = c_{33}{}^{E} + e_{33}^{2}/\varepsilon_{33}{}^{S}$, whereas the agreement between the corresponding elastic constants at constant electric field $c_{33}{}^{E}$ is good, at least between resonance and RUS measurements. Unlike the previous cases, these constants are related to the propagation of longitudinal waves and do not show the technical difficulties mentioned above. Given that measurements are performed in different frequency ranges (from 100 to 400 kHz for RUS, about 1 MHz and 10 GHz for the impedance measurements and Brillouin scattering respectively), this seems to point to a frequency dependence of the ratio $e_{33}^{2}/\varepsilon_{33}{}^{S}$. This is consistent with the hypotheses expressed in the previous Brillouin scattering studies of $BaTiO_3$ [8] and $KNbO_3$ [10]: the authors had pointed out the difficulties arising from the piezoelectric properties of the crystals, and had suggested a frequency dependence of the dielectric constant $\varepsilon_{33}{}^{S}$. Independent measurements of dielectric constants in the GHz range might help to clarify this point.

5. Conclusion

We have compared measurements of the piezoelastic tensor by the resonance methods, Brillouin scattering and resonant ultrasound spectroscopy (RUS). Despite relatively high uncertainties affecting the results from the resonance methods, the agreement is found to be good for many elastic constants. However, the agreement is not satisfactory for the constants associated to propagation of shear waves ($c_{66}{}^{E}$ and $c_{44}{}^{E}$), which can be accounted for by imperfections of the sample used for RUS and specific difficulties of shear resonators in the resonance methods. The latter is especially important to bear in mind when using the piezoelastic tensor of a single domain state as input data for the calculation of macroscopic properties in morphotropic multidomain crystals. A significant discrepancy is also found for the hardened elastic constants $c_{33}{}^{D}$ and seems to point to a frequency dependence of the dielectric constant.

References

[1] S.E. Park, T.R. Shrout, IEEE Trans. Ultrason. Ferroelectr. Freq. Control 44 (1997) 1997.
[2] A.E. Renault, H. Dammak, G. Calvarin, M. Pham Thi, P. Gaucher, Jpn. J. Appl. Phys. 41 (2002) 3846.
[3] J.J. Lima-Silva, I. Guedes, J. Mendes Filho, A.P. Ayala, M.H. Lente, J.A. Eiras, D. Garcia, Solid State Commun. 131 (2004) 111.
[4] H. Dammak, M. Guennou, C. Ketchazo, M. Pham Thi, F. Brochin, T. Delaunay, P. Gaucher, E. Le Clézio, G. Feuillard, Proceedings of the 15th IEEE International Symposium on Applications of Ferroelectrics (2006) p. 249.
[5] X. Geng, T.A. Ritter, S.E. Park, Proceedings of the IEEE Ultrasonics Symposium (1998) p. 571.
[6] IEEE, ANSI/IEEE Standard 176, 1987.
[7] R. Vacher, L. Boyer, Phys. Rev. B 6 (1972) 639.
[8] Z. Li, S.K. Chan, M.H. Grimsditch, E.S. Zouboulis, J. Appl. Phys. 70 (1991) 7327.
[9] A.G. Kalinichev, J.D. Bass, B.N. Sun, D.A. Payne, J. Mater. Res. 12 (1997) 2623.
[10] A.G. Kalinichev, J.D. Bass, C.S. Zha, P. Han, D.A. Payne, J. Appl. Phys. 74 (1993) 6603.
[11] M. Ahart, A. Asthagiri, P. Dera, H.K. Mao, R.E. Cohen, R.J. Hemley, Appl. Phys. Lett. 88 (2006) 042908.
[12] Z. Xu, G.G. Siu, Y. Liu, H. Luo, J. Appl. Phys. 101 (2007) 026113.
[13] T. Delaunay, E. Le Clézio, M. Guennou, H. Dammak, M. Pham Thi, G. Feuillard, IEEE Trans. Ultrason. Ferroelectr. Freq. Control 55 (2008) 476.
[14] S. Zhang, L. Lebrun, C.A. Randall, T.R. Shrout, Phys. Status Solidi (A) 202 (2005) 151.
[15] W. Jiang, R. Zhang, B. Jiang, W. Cao, Ultrasonics 41 (2003) 55.
[16] W. Cao, S. Zhu, B. Jiang, J. Appl. Phys. 83 (1998) 4415.

Please cite this article in press as: M. Guennou, H. Dammak, et al., Electromechanical properties of single domain PZN–12%PT measured by three different methods, Solid State Sci. (2009), doi:10.1016/j.solidstatesciences.2009.03.026